Ribosome structure reveals preservation of active sites in the presence of a P-site wobble mismatch

Egor Svidritskiy[1] and **Andrei A. Korostelev**[1,*]

[1]RNA Therapeutics Institute, Department of Biochemistry and Molecular Pharmacology, University of Massachusetts Medical School, 368 Plantation St., Worcester, MA 01605, USA

Abstract

Translation initiation in the P site occasionally occurs at atypical (non-AUG) start codons, including those forming a mismatch in the third (wobble) position. During elongation, however, a pyrimidine-pyrimidine wobble mismatch may trigger a translation quality control mechanism, whereby the P-site mismatch is thought to perturb the downstream A-site codon or the decoding center, thereby reducing translation fidelity and inducing termination of aberrant translation. We report a crystal structure of the 70S initiation complex containing an AUC codon in the ribosomal P site. Remarkably, the ribosome stabilizes the mismatched codon-anticodon helix, arranging a normally disruptive cytosine-cytosine pair into a Watson-Crick-like conformation. Translation-competent conformations of the tRNA, mRNA and decoding center suggest that a P-site wobble-position mismatch in the 70S initiation complex does not pre-arrange the mRNA or decoding center to favor subsequent miscoding events.

INTRODUCTION

Protein synthesis, or translation, usually initiates at an AUG start codon of a messenger RNA (mRNA). The AUG start codon forms three Watson-Crick base pairs with the CAU anticodon of initiator transfer RNA (N-formylmethionyl-tRNA^{fMet} in bacteria and methionyl-tRNA$^{Met}_i$ in eukaryotes) in the P (peptidyl-tRNA) site of the ribosome (Aitken and Lorsch, 2012; Simonetti et al., 2009). Ribosomes can, however, initiate translation on codons other than AUG in all three domains of life. The most common non-AUG codons contain a mismatch in the first position (Ivanov et al., 2011; Rocha et al., 1999; Torarinsson et al., 2005; Vellanoweth and Rabinowitz, 1992). A smaller subset of mRNAs contains a mismatch in the second or third position. In *E. coli*, the efficiency of initiation at AUA, AUU, and AUC wobble-position mismatched codons is at least 5% of that of AUG-dependent initiation (Romero and Garcia, 1991). An AUC codon within the open reading

*Correspondence: andrei.korostelev@umassmed.edu (A.A.K)..

frame can be used as an alternative initiation codon (Chalut and Egly, 1995). In eukaryotes, a subset of mRNAs also initiate at an AUC codon (Ivanov et al., 2011; Olsen, 1987). Whereas non-AUG initiation has been shown to be remarkably prevalent (Ingolia et al., 2009; Ivanov et al., 2011), the structural basis of recognition of non-AUG initiation codons by the initiator tRNA in the P site is unknown.

During translation elongation, the decoding of elongator tRNAs takes place in the A (aminoacyl-tRNA) site. Here, the first two nucleotides of each codon form Watson-Crick base-pair interactions with the last two nucleotides of a cognate tRNA anticodon, stabilized by interactions with universally conserved nucleotides of 16S ribosomal RNA A1492 and A1493 (*E. coli* numbering) (Demeshkina et al., 2012; Ogle et al., 2001; Ogle et al., 2003). The third nucleotide of the codon, called the wobble position, can form a non-Watson-Crick base pair with the first nucleotide of the tRNA anticodon. Wobble pairs, including purine-purine (e.g., inosine-adenosine) or purine-pyrimidine (e.g., guanosine-uridine), can adopt a Watson-Crick-like geometry (Murphy and Ramakrishnan, 2004) or non-Watson-Crick geometry characteristic of the G-U pair (Demeshkina et al., 2012). The relaxed base-pair criteria at the wobble position results in a redundant genetic code, in which multiple codons encode the same amino acid (Crick, 1966).

The relaxed base-pairing criteria at the wobble position can, however, lead to miscoding by near-cognate tRNAs (Woese, 1967; Zhang et al., 2013). These include tRNAs that form pyrimidine-pyrimidine pairs, which are less energetically stable than wobble pairs (Davis and Znosko, 2007; Gralla and Crothers, 1973; Kierzek et al., 1999). Such tRNAs can bind the A site under cellular stress conditions. During asparagine starvation, for example, the ribosome misreads the AAU and AAC asparagine codons by accommodation of tRNA^{Lys}, whose anticodons (CUU or UUU) differ from tRNA^{Asn} anticodon sequences (AUU or GUU) at the wobble position (Johnston et al., 1984; Parker et al., 1980; Parker et al., 1978). A similar phenomenon was observed in the case of histidine codons, and was also interpreted as a result of a pyrimidine-pyrimidine miscoding in the wobble position (O'Farrell, 1978). In "relaxed" bacterial strains, which are incapable of initiating nutrient-deprivation-caused stringent response (Laffler and Gallant, 1974; Stent and Brenner, 1961), pyrimidine-pyrimidine miscoding upon asparagine starvation becomes nearly as frequent as correct pairing (Johnston et al., 1984; Parker et al., 1980).

Following translocation, a wobble-mismatch-containing peptidyl-tRNA in the P site can dramatically reduce the fidelity of subsequent aminoacyl-tRNA selection, such that the A site accommodates a near-cognate tRNA almost as efficiently as a cognate tRNA (Zaher and Green, 2010). Furthermore, the loss of decoding fidelity in mismatched complexes results in stop-codon-independent termination by release factor 2 (RF2), enhanced by the auxiliary release factor RF3 (Petropoulos et al., 2014; Zaher and Green, 2009). Stop-codon-independent termination in *E. coli* was proposed to underlie a quality control, which aborts protein synthesis if amino acids are misincorporated (Zaher and Green, 2009). Miscoding in the A site caused by a pyrimidine-pyrimidine mismatch in the P site is thought to result from conformational changes in the downstream A-site codon or the ribosomal decoding center. Kinetic studies suggest that tRNA^{Lys} (UUU) miscoding of an AAU asparagine codon (i.e., U-U wobble mismatch) is mechanistically similar to miscoding caused by streptomycin

(Gromadski and Rodnina, 2004; Zaher and Green, 2010). Streptomycin binds the decoding center and induces significant conformational changes, including the shift of the 16S rRNA nucleotides A1492 and A1493, which stabilize the tRNA-mRNA helix (Demirci et al., 2013). Whether a pyrimidine-pyrimidine wobble mismatch induces structural changes in the bacterial 70S ribosome, however, has not been tested.

To gain insight into non-AUG initiation and structural effects of a pyrimidine-pyrimidine mismatch, we have determined a 3.6 Å crystal structure of the bacterial 70S initiation complex containing a cytosine-cytosine (C-C) mismatch in the wobble position of the P site (Fig. 1). We chose a C-C mismatch, because it is the weakest pyrimidine-pyrimidine pair, which exhibits deviation from base-pair co-planarity (Tavares et al., 2009) and imparts the most instability to nucleic acid structures in solution (Fig. 2A; (Battle and Doudna, 2002; Gralla and Crothers, 1973)).

Results

We report a crystal structure of the *Thermus thermophilus* 70S ribosome containing initiator tRNA^{fMet} (CAU anticodon) bound with an mRNA containing an AUC codon in the P site (Fig. 1; Table 1). The mRNA (5′-GGCAAGGAGGUAAAA**AUC**UAAAAAAAA-3′) included a 5′ Shine-Dalgarno sequence (Dalgarno and Shine, 1973; Shine and Dalgarno, 1974), followed by a four-nucleotide linker, to help position the AUC codon in the ribosomal P site (Korostelev et al., 2007; Yusupova et al., 2006). In the resulting structure, well-ordered mRNA nucleotides were modeled in the E (exit), P and A sites, whereas the flanking mRNA regions, including the Shine-Dalgarno sequence, were not modeled due to disorder (Laurberg et al., 2008; Polikanov et al., 2014; Selmer et al., 2006; Svidritskiy et al., 2013). We also used *E. coli* release factor 1 (RF1) and blasticidin S in crystallization solutions, hypothesizing that they could help stabilize the complex. However, neither RF1 nor blasticidin S was found in the resulting Fourier difference maps. The lack of binding could be due to competition between these two molecules (Svidritskiy et al., 2013), and/or because they were not added in cryo-protection buffer-exchange steps, which may have resulted in ligand or factor dissociation (Gagnon et al., 2012).

Interactions in the P site of the 30S subunit

The 70S ribosome structure containing the C-C mismatch is globally similar to the canonical 70S initiation complex containing tRNA^{fMet} bound to an AUG codon (Jenner et al., 2010; Svidritskiy et al., 2013), indicating that the wobble-position C-C mismatch does not affect the conformations of the ribosome or individual subunits during initiation.

The mRNA-tRNA duplex in the P site adopts a nearly perfect A-form conformation (Fig. 2B). The phosphate backbones of both the mRNA and tRNA are positioned similarly to those in the 70S structures containing the start AUG codon and tRNA^{fMet} (Jenner et al., 2010; Svidritskiy et al., 2013). The mRNA nucleotides A1, U2, and C3 face the tRNA anticodon nucleotides U36, A35, and C34, respectively (Figs. 1B, 1C). The first two nucleotides of the P-site codon form canonical Watson-Crick base pairs. The cytosine in the third position of the codon is nearly coplanar to C34 of the tRNA anticodon, similar to a canonical Watson-Crick base pair (Korostelev et al., 2006; Selmer et al., 2006). The

positions of the well-resolved cytidines suggest that the bases interact via weak hydrogen bonding between the exocyclic amino group of the tRNA cytosine and the N3 atom of the mRNA cytosine (Fig. 1C).

Base stacking and backbone interactions stabilize the C-C mismatch pair (Fig. 1C). The universally conserved nucleotide C1400 of the 16S rRNA renders the stacking foundation for both cytosines. The ribose of C1400 forms the platform for the base of C3, while the base of C1400 stacks on the cytosine of C34. The U-A base pair at the second position of the codon forms base stacking interactions on the opposite side of the C-C mismatch. The distances between the planes formed by stacked nucleotides U2-A35, C3-C34 and C1400 are ~3.5 Å or less, similar to those for the stacked base pairs of an A-form helix (Fig. 2B). This further indicates that base-pair planarity parameters, such as buckle and propeller dihedral angles, for the cytosine pair are close to those for co-planar Watson-Crick base pairs. The nucleic acid backbones of the mismatch cytidines are also stabilized by interactions with 16S rRNA nucleotides. The phosphate group of C3 is held in place by the amino groups of the conserved C1402 and C1403, while the ribose of C34 stacks on the base of G966 (Fig. 1C).

Conformation of the downstream A-site codon and decoding center

In previous crystal structures of ribosome complexes formed with fully cognate tRNAs or release factors, the path of mRNA kinks sharply between the P and A sites; the kink is stabilized by a magnesium ion coordinating with the backbone of mRNA and 16S rRNA (Fig. 3; Selmer et al., 2006). The mRNA nucleotides adopt similar conformations in the absence (Jenner et al., 2010) or presence (Selmer et al., 2006) of cognate tRNA in the A site, although the A-site codon and the ribosomal nucleotides of the decoding center are usually less well resolved in crystal structures determined in the absence of A-site ligands, such as tRNA, release factors or aminoglycoside antibiotics (Bulkley et al., 2014; Korostelev et al., 2006; Schuwirth et al., 2005). Previous structural studies have shown that the nucleotides of the ribosomal decoding center undergo structural rearrangements to stabilize the codon interactions with aminoacyl-tRNA (Fig. 3A; (Ogle et al., 2001; Selmer et al., 2006)) or release factors (Fig. 3B; (Jin et al., 2010; Korostelev et al., 2008; Korostelev et al., 2010; Laurberg et al., 2008; Weixlbaumer et al., 2008)). Because the P-site wobble position is immediately adjacent to the kink between the P and A codons, a mismatch pair in the wobble position was predicted to perturb the conformation of the A-site codon or decoding center, resulting in reduced translation fidelity (Zaher and Green, 2010).

In our 70S structure, we find that even in the presence of a P-site wobble-position mismatch, the mRNA path in the A site does not deviate from the path observed in structures formed with a fully cognate tRNA in the P site. The mRNA used in this study contained a UAA codon following the mismatch AUC codon. In an unbiased Fourier difference density map, strong density for the first two nucleotides (U4 and A5) of the A-site codon reveals that the mRNA forms a sharp kink - between the P- and A-site codons - which is stabilized by a magnesium ion (Figs. 3C,D), as in crystal structures of cognate complexes (Jenner et al., 2010; Selmer et al., 2006).

Since the UAA codon signals translation termination, we have compared our structure to 70S crystal structures in which the A-site UAA codon is bound by RF1 or RF2 release factor (Korostelev et al., 2008; Laurberg et al., 2008). Release factors induce a conformational change in the A-site codon, displacing the first two nucleotides by more than 2 Å from their corresponding "sense-codon" positions and unstacking the third nucleotide from the first two bases. In our structure, however, the first two nucleotides of the A-site codon adopt the positions distinct from those in the RF1- and RF2-bound complexes. Specifically, their placement is nearly identical to that of sense-codon nucleotides. The density for the third nucleotide is weak, consistent with conformational flexibility of the third nucleotide, as reported by the crystals structures containing sense codons in the A site (e.g. PDB IDs 3I9B, 3I9D, 4QCY and 4QD0 (Jenner et al., 2010; Polikanov et al., 2014)). Thus, although the UAA codon encodes a termination signal, its position and conformation in the absence of the release factors are for the most part similar to those of a sense codon.

To visualize the effect of the C-C mismatch on the A-site conformation in detail, we compared our structure with the recent 70S initiation structure, containing the same mRNA sequence aside from a cognate AUG codon in the P site (Svidritskiy et al., 2013). We found that the A-site nucleotide densities of the cognate complex and the mismatch complex are nearly equivalent. In line with the absence of large conformational rearrangements in the P- and A-site codons, the structure of the ribosomal decoding center is also unchanged. Specifically, nucleotides A1492 and A1493 of 16S rRNA, which are involved in tRNA decoding via A-minor interactions with the codon-anticodon helix (Fig. 3A; (Demeshkina et al., 2012; Ogle et al., 2001; Ogle et al., 2003)), in our structure are docked inside helix 44 and contact the tip of helix 69 of 23S rRNA (residue A1913), as in cognate complexes with a vacant A site (Bulkley et al., 2014; Jenner et al., 2010; Svidritskiy et al., 2013). Although electron density indicates that these nucleotides in our and cognate complexes are more dynamic than in the complexes containing an A-site ligand, it is clear that they are not pre-ordered (Fig. 3C) for formation of a tRNA-bound or RF2-bound states, in both of which A1492 is flipped out of helix 44 to interact with G530 (Figs. 3A,B).

In summary, our structure shows that despite a potentially destabilizing C-C mismatch immediately before the A-site codon, the A-site codon and decoding center adopt a canonical conformation observed in 70S complexes formed with a cognate P-site codon.

Discussion

In this work, we examined the structural consequences of a pyrimidine-pyrimidine mismatch in the wobble position of the P site. Our findings contrast with solution studies of structured nucleic acids containing a C-C mismatch. C-C mismatches impart a large energetic penalty of up to ~11 kcal/mol (Battle and Doudna, 2002) and destabilize secondary and tertiary structures (Battle and Doudna, 2002; Cate et al., 1996; Gralla and Crothers, 1973). In an NMR structure of an RNA hairpin (Tavares et al., 2009), for example, the mismatched cytosines are out of plane, dramatically widening the major groove and distorting the helical axis by up to 45° (Fig. 2A). In our 70S ribosome structure, however, the nearly coplanar orientation and relative positions of C3 and C34 closely resemble the mismatched C-C pairs observed in the crystal structure of an A-form helix formed by CCG-repeat RNA molecules

(Fig. 2B). The A-helix conformation in the (CCG)$_n$ duplex is likely stabilized by the continuous base stacking owing to crystal packing, and locally by the stacking with guanosine-cytosine base pairs on either side of the C-C mismatch (Kiliszek et al., 2012). Superposition of the (CCG)$_n$ structure with the codon-anticodon helix in our 70S structure shows that the U2-A35 pair and C1400, which sandwich the C-C pair in the ribosome, provide a stacking foundation somewhat similar to that rendered by the C-G and G-C Watson-Crick pairs flanking the C-C mismatch in the A-form helix (Fig. 2B). The notable difference between these two structures is that the ribosome does not contain a long system of stacked and base-paired nucleotides as in the (CCG)$_n$ helix. Instead, universally conserved nucleotides of the small ribosomal subunit provide a scaffold that stabilizes both the backbone and bases of the wobble-position nucleotides, allowing the non-canonical C-C pair to adopt a nearly coplanar conformation that resembles a Watson-Crick pair. The initiator-tRNA-specific properties, such as the three consecutive G-C pairs that are conserved in the anticodon stem and interact with the conserved 16S nucleotides G1338 and A1339 (Korostelev et al., 2006; Selmer et al., 2006), further contribute to the stability of initiation complexes (Dong et al., 2014; Lancaster and Noller, 2005).

The conformation of the A site, immediately downstream from the C-C mismatch, is poised to continue normal translation rather than to accommodate subsequent anomalies, such as reduced fidelity of tRNA selection and RF2-induced stop-codon-independent termination. Thus, the P-site wobble-position mismatch does not pre-arrange the mRNA or decoding center for miscoding, rendering a non-AUG initiation complex translation competent. It is notable that the wobble mismatch in such initiation complexes occurs in the context of the A-U and U-A pairs formed at the first and second positions of the codon, respectively. These base pairs confer low structural stability to a double helix, and the neighboring C-C mismatch is expected to substantially destabilize the base-pairing interactions in the short codon-anticodon helix. In fact, studies on helix-forming oligonucleotides have shown that insertion of the C-C mismatch in the middle of a A-U- and U-A-paired double helix completely abrogates a 10-base-pair-long double helix formation at 25°C (Gralla and Crothers, 1973). Our structure demonstrates the critical role of the ribosomal P site in providing a highly stable scaffold to stabilize even weak mRNA-tRNA interactions, in keeping with the role of the P site in establishing and maintaining an mRNA reading frame.

Our structure also provides a framework for understanding the mechanism of the post-peptidyl-transfer quality control during elongation. The preservation of the A and P site conformations appears to argue against a structural mechanism, in which P-site wobble mismatch induces conformational changes to the mRNA or decoding center to pre-arrange the decoding center for miscoding. We note that only a U-U mismatch has been studied in detail biochemically (Petropoulos et al., 2014; Zaher and Green, 2009; Zaher and Green, 2010); kinetic analyses of translational infidelity are lacking for other mismatches. A U-U mismatch is favorable for RNA helix stability (Mathews et al., 2004; Schroeder et al., 1996) since uracil pairs can form direct and water-mediated hydrogen bonds in RNA duplexes ((Kiliszek and Rypniewski, 2014) and references therein; (Zoll et al., 2007)). A U-U pair also adopts a coplanar Watson-Crick-like conformation and does not alter the A-form geometry of an RNA helix in solution (Zoll et al., 2007). A U-U pair is the most thermodynamically stable and most frequent pyrimidine-pyrimidine mismatch in naturally

occurring RNA structures (Davis and Znosko, 2007; Kierzek et al., 1999). These observations, therefore, suggest that a U-U mismatch is even less likely than a C-C mismatch to induce substantial conformational changes that pre-arrange the A site for miscoding.

Rather than pre-arranging the mRNA or decoding center for miscoding, it is possible that the P-site mismatch interferes with EF-Tu-dependent aminoacyl-tRNA loading and release-factor binding at the A site. For example, the P-site mismatch could affect transient conformations, normally sampled during aminoacyl-tRNA or release-factor binding, thus altering the energy landscape of A-site accommodation. This mechanistic model is consistent with kinetic studies that examined how a P-site mismatch in elongation complexes influences the selection of near-cognate aminoacyl-tRNA (Zaher and Green, 2010). The association rate (k_{on}) of a near-cognate ternary complex (aa-tRNA*EF-Tu*GTP) with the A site was not influenced by the mismatch, suggesting that mismatched and matched complexes share similar association mechanisms. By contrast, the dissociation rate (k_{off}) of near-cognate ternary complex from mismatched P-site ribosomes was reduced ~100-fold relative to that of near-cognate ternary complex from a matched P-site ribosome, largely accounting for the reduced fidelity of aa-tRNA selection. Moreover, the rate of GTP hydrolysis by EF-Tu is increased on mismatched complexes by ~10-fold, enhancing the efficiency of near-cognate tRNA accommodation. Together, these biochemical studies and our structure suggest that the mismatch-induced effects take place in the course of interaction of a near-cognate ligand with the A site.

Additional work is required to test the proposed post-peptidyl-transfer quality control mechanism. While our 70S initiation complex provides, to our knowledge, the initial visualization of the wobble mismatch effects, structural studies of *bona fide* elongation complexes prone to translational infidelity are necessary to capture states along the A-site misincorporation trajectory. Furthermore, the extent to which mismatch-induced quality control is present and mechanistically conserved among bacteria remains to be established. The universal conservation of the ribosome decoding-center structure and decoding mechanism (Ogle et al., 2001; Wilson and Doudna Cate, 2012) suggests mechanistic similarity for the quality control. However, strain-specific variability in the termination aspect of the quality control in *E. coli* (O'Connor, 2015) and the strong dependence on the non-essential release factor RF3, which is absent from some bacteria including *T. thermophilus*, suggest that the termination of aberrant translation might only be employed or mechanistically conserved in a subset of bacteria. In summary, further genetic, structural and biochemical studies involving U-U, C-C and other mismatches are required to delineate the affected A-site accommodation steps, and determine the extent to which tRNA miscoding and termination are shared by P-site mismatches.

Experimental Procedures

Crystal Structure Determination

70S ribosomes were purified from *Thermus thermophilus* HB27 as described (Laurberg et al., 2008). To assemble the 70S complex for crystallization, 4 μM 70S ribosomes were incubated with the 2.2-fold molar excess of tRNA^fMet (Chemical Block), 3-fold molar

excess mRNA (5′-GGCAAGGAGGUAAAA**AUC**UAAAAAAAA-3′, IDT) in a buffer containing 25 mM Tris·acetate (pH 7.0), 50 mM potassium acetate, 10 mM ammonium acetate, and 10 mM magnesium acetate (all concentrations in the final solution). We have also added 3-fold molar excess of *E. coli* release factor 1 and 650 μM blasticidin S during the complex formation, however neither RF1 nor blasticidin S was found in the resulting Fourier difference maps. Crystallization drops contained 3.1 μL of the 70S·mRNA·tRNA^{fMet} complex mixed with 3.1 μL crystallization buffer containing 0.1 M Tris·HCl (pH 7.5), 4% (vol/vol) PEG 20000, 8% (vol/vol) 2-Methyl-2,4-pentanediol, and 0.2 M KSCN. Crystallization was performed by hanging-drop vapor diffusion method using 300 μL of 0.5–0.7 M NaCl as reservoir solution. Crystals were cryo-protected in four steps, as described (Svidritskiy et al., 2013) and flash-frozen by plunging into liquid nitrogen.

Diffraction data were collected at beam line 23ID-B at the Advanced Photon Source at Argonne National Laboratory using MARmosaic 300 CCD detector at an X-ray wavelength of 1.033 Å and an oscillation angle of 0.2°. The final data set was obtained by merging three datasets collected from two crystals. The data were integrated, merged and scaled using XDS (Kabsch, 2010); 1% of reflections were used as test-set (R^{free} set). As a starting model for molecular replacement, the crystal structure of blasticidin-S-bound ribosome obtained from the same crystal form (Svidritskiy et al., 2013) was used, excluding blasticidin S, mRNA and anticodon stem-loop of the P-site tRNA. Models of ribosomal proteins L6 and L18, for which additional density was observed in our maps in the N- and C-terminal regions, were adopted from a 70S ribosome structure by Polikanov and colleagues (Polikanov et al., 2014). The nucleotides of tRNA, mRNA and the decoding center were built into the initial Fo-Fc and 3Fo-2Fc difference maps. PHENIX (Adams et al., 2002) and RSRef (Korostelev et al., 2002) were used for reciprocal-space and local-real-space simulated-annealing refinements (Laurberg et al., 2008; Svidritskiy et al., 2014), yielding the final structure with R^{work}/R^{free} of 0.268/0.287 and good stereochemical parameters (Table 1). Non-crystallographic symmetry restraints were employed during refinement for the two ribosomes in the asymmetric unit (Laurberg et al., 2008). Fo-Fc and 2Fo-Fc density maps were calculated in PHENIX and shown at σ=1.5 (Fig. 3D) and σ=1.0 (Fig. 1B), respectively. PyMOL (DeLano, 2002) was used for figure rendering and structure superpositions. The atomic coordinates and structure factors are available in the Protein Data Bank (PDB ID code 5D8B).

Acknowledgments

REFERENCES

The CCP4 suite: programs for protein crystallography. Acta Crystallogr D Biol Crystallogr. 1994; 50:760–763. [PubMed: 15299374]

Aitken CE, Lorsch JR. A mechanistic overview of translation initiation in eukaryotes. Nat Struct Mol Biol. 2012; 19:568–576. [PubMed: 22664984]

Battle DJ, Doudna JA. Specificity of RNA-RNA helix recognition. Proc Natl Acad Sci U S A. 2002; 99:11676–11681. [PubMed: 12189204]

Bulkley D, Brandi L, Polikanov YS, Fabbretti A, O'Connor M, Gualerzi CO, Steitz TA. The antibiotics dityromycin and GE82832 bind protein S12 and block EF-G-catalyzed translocation. Cell Rep. 2014; 6:357–365. [PubMed: 24412368]

Cate JH, Gooding AR, Podell E, Zhou K, Golden BL, Kundrot CE, Cech TR, Doudna JA. Crystal structure of a group I ribozyme domain: principles of RNA packing. Science. 1996; 273:1678–1685. [PubMed: 8781224]

Chalut C, Egly JM. AUC is used as a start codon in Escherichia coli. Gene. 1995; 156:43–45. [PubMed: 7537704]

Crick FH. Codon--anticodon pairing: the wobble hypothesis. J Mol Biol. 1966; 19:548–555. [PubMed: 5969078]

Davis AR, Znosko BM. Thermodynamic characterization of single mismatches found in naturally occurring RNA. Biochemistry. 2007; 46:13425–13436. [PubMed: 17958380]

Demeshkina N, Jenner L, Westhof E, Yusupov M, Yusupova G. A new understanding of the decoding principle on the ribosome. Nature. 2012; 484:256–259. [PubMed: 22437501]

Demirci H, Murphy F. t. Murphy E, Gregory ST, Dahlberg AE, Jogl G. A structural basis for streptomycin-induced misreading of the genetic code. Nat Commun. 2013; 4:1355. [PubMed: 23322043]

Dong J, Munoz A, Kolitz SE, Saini AK, Chiu WL, Rahman H, Lorsch JR, Hinnebusch AG. Conserved residues in yeast initiator tRNA calibrate initiation accuracy by regulating preinitiation complex stability at the start codon. Genes Dev. 2014; 28:502–520. [PubMed: 24589778]

Gagnon MG, Seetharaman SV, Bulkley D, Steitz TA. Structural basis for the rescue of stalled ribosomes: structure of YaeJ bound to the ribosome. Science. 2012; 335:1370–1372. [PubMed: 22422986]

Gralla J, Crothers DM. Free energy of imperfect nucleic acid helices. 3. Small internal loops resulting from mismatches. J Mol Biol. 1973; 78:301–319. [PubMed: 4747633]

Gromadski KB, Rodnina MV. Streptomycin interferes with conformational coupling between codon recognition and GTPase activation on the ribosome. Nat Struct Mol Biol. 2004; 11:316–322. [PubMed: 15004548]

Ingolia NT, Ghaemmaghami S, Newman JR, Weissman JS. Genome-wide analysis in vivo of translation with nucleotide resolution using ribosome profiling. Science. 2009; 324:218–223. [PubMed: 19213877]

Ivanov IP, Firth AE, Michel AM, Atkins JF, Baranov PV. Identification of evolutionarily conserved non-AUG-initiated N-terminal extensions in human coding sequences. Nucleic Acids Res. 2011; 39:4220–4234. [PubMed: 21266472]

Jenner LB, Demeshkina N, Yusupova G, Yusupov M. Structural aspects of messenger RNA reading frame maintenance by the ribosome. Nat Struct Mol Biol. 2010; 17:555–560. [PubMed: 20400952]

Jin H, Kelley AC, Loakes D, Ramakrishnan V. Structure of the 70S ribosome bound to release factor 2 and a substrate analog provides insights into catalysis of peptide release. Proc Natl Acad Sci U S A. 2010; 107:8593–8598. [PubMed: 20421507]

Johnston TC, Borgia PT, Parker J. Codon specificity of starvation induced misreading. Mol Gen Genet. 1984; 195:459–465. [PubMed: 6590943]

Karplus PA, Diederichs K. Linking crystallographic model and data quality. Science. 2012; 336:1030–1033. [PubMed: 22628654]

Kierzek R, Burkard ME, Turner DH. Thermodynamics of single mismatches in RNA duplexes. Biochemistry. 1999; 38:14214–14223. [PubMed: 10571995]

Kiliszek A, Kierzek R, Krzyzosiak WJ, Rypniewski W. Crystallographic characterization of CCG repeats. Nucleic Acids Res. 2012; 40:8155–8162. [PubMed: 22718980]

Kiliszek A, Rypniewski W. Structural studies of CNG repeats. Nucleic Acids Res. 2014; 42:8189–8199. [PubMed: 24939898]

Korostelev A, Asahara H, Lancaster L, Laurberg M, Hirschi A, Zhu J, Trakhanov S, Scott WG, Noller HF. Crystal structure of a translation termination complex formed with release factor RF2. Proc Natl Acad Sci U S A. 2008; 105:19684–19689. [PubMed: 19064930]

Korostelev A, Trakhanov S, Laurberg M, Noller HF. Crystal structure of a 70S ribosome-tRNA complex reveals functional interactions and rearrangements. Cell. 2006; 126:1065–1077. [PubMed: 16962654]

Korostelev A, Zhu J, Asahara H, Noller HF. Recognition of the amber UAG stop codon by release factor RF1. Embo J. 2010

Laffler T, Gallant JA. Stringent control of protein synthesis in E. coli. Cell. 1974; 3:47–49. [PubMed: 4607106]

Lancaster L, Noller HF. Involvement of 16S rRNA nucleotides G1338 and A1339 in discrimination of initiator tRNA. Mol Cell. 2005; 20:623–632. [PubMed: 16307925]

Laurberg M, Asahara H, Korostelev A, Zhu J, Trakhanov S, Noller HF. Structural basis for translation termination on the 70S ribosome. Nature. 2008; 454:852–857. [PubMed: 18596689]

Mathews DH, Disney MD, Childs JL, Schroeder SJ, Zuker M, Turner DH. Incorporating chemical modification constraints into a dynamic programming algorithm for prediction of RNA secondary structure. Proc Natl Acad Sci U S A. 2004; 101:7287–7292. [PubMed: 15123812]

Murphy, F. V. t.; Ramakrishnan, V. Structure of a purine-purine wobble base pair in the decoding center of the ribosome. Nat Struct Mol Biol. 2004; 11:1251–1252. [PubMed: 15558050]

O'Connor M. Interactions of release factor RF3 with the translation machinery. Mol Genet Genomics. 2015; 290:1335–1344. [PubMed: 25636454]

O'Farrell PH. The suppression of defective translation by ppGpp and its role in the stringent response. Cell. 1978; 14:545–557. [PubMed: 357011]

Ogle JM, Brodersen DE, Clemons WM Jr. Tarry MJ, Carter AP, Ramakrishnan V. Recognition of cognate transfer RNA by the 30S ribosomal subunit. Science. 2001; 292:897–902. [PubMed: 11340196]

Ogle JM, Carter AP, Ramakrishnan V. Insights into the decoding mechanism from recent ribosome structures. Trends Biochem Sci. 2003; 28:259–266. [PubMed: 12765838]

Olsen O. Yeast cells may use AUC or AAG as initiation codon for protein synthesis. Carlsberg Res Commun. 1987; 52:83–90.

Parker J, Johnston TC, Borgia PT. Mistranslation in cells infected with the bacteriophage MS2: direct evidence of Lys for Asn substitution. Mol Gen Genet. 1980; 180:275–281. [PubMed: 6780757]

Parker J, Pollard JW, Friesen JD, Stanners CP. Stuttering: high-level mistranslation in animal and bacterial cells. Proc Natl Acad Sci U S A. 1978; 75:1091–1095. [PubMed: 349556]

Petropoulos AD, McDonald ME, Green R, Zaher HS. Distinct roles for release factor 1 and release factor 2 in translational quality control. J Biol Chem. 2014; 289:17589–17596. [PubMed: 24798339]

Polikanov YS, Steitz TA, Innis CA. A proton wire to couple aminoacyl-tRNA accommodation and peptide-bond formation on the ribosome. Nat Struct Mol Biol. 2014; 21:787–793. [PubMed: 25132179]

Rocha EP, Danchin A, Viari A. Translation in Bacillus subtilis: roles and trends of initiation and termination, insights from a genome analysis. Nucleic Acids Res. 1999; 27:3567–3576. [PubMed: 10446248]

Romero A, Garcia P. Initiation of translation at AUC, AUA and AUU codons in Escherichia coli. FEMS Microbiol Lett. 1991; 68:325–330. [PubMed: 1687139]

Schroeder S, Kim J, Turner DH. G.A and U.U mismatches can stabilize RNA internal loops of three nucleotides. Biochemistry. 1996; 35:16105–16109. [PubMed: 8973181]

Schuwirth BS, Borovinskaya MA, Hau CW, Zhang W, Vila-Sanjurjo A, Holton JM, Cate JH. Structures of the bacterial ribosome at 3.5 A resolution. Science. 2005; 310:827–834. [PubMed: 16272117]

Selmer M, Dunham CM, Murphy FV, Weixlbaumer A, Petry S, Kelley AC, Weir JR, Ramakrishnan V. Structure of the 70S ribosome complexed with mRNA and tRNA. Science. 2006; 313:1935–1942. [PubMed: 16959973]

Simonetti A, Marzi S, Jenner L, Myasnikov A, Romby P, Yusupova G, Klaholz BP, Yusupov M. A structural view of translation initiation in bacteria. Cell Mol Life Sci. 2009; 66:423–436. [PubMed: 19011758]

Stent GS, Brenner S. A genetic locus for the regulation of ribonucleic acid synthesis. Proc Natl Acad Sci U S A. 1961; 47:2005–2014. [PubMed: 13916843]

Svidritskiy E, Ling C, Ermolenko DN, Korostelev AA. Blasticidin S inhibits translation by trapping deformed tRNA on the ribosome. Proc Natl Acad Sci U S A. 2013; 110:12283–12288. [PubMed: 23824292]

Tavares TJ, Beribisky AV, Johnson PE. Structure of the cytosine-cytosine mismatch in the thymidylate synthase mRNA binding site and analysis of its interaction with the aminoglycoside paromomycin. RNA. 2009; 15:911–922. [PubMed: 19329536]

Torarinsson E, Klenk HP, Garrett RA. Divergent transcriptional and translational signals in Archaea. Environ Microbiol. 2005; 7:47–54. [PubMed: 15643935]

Vellanoweth RL, Rabinowitz JC. The influence of ribosome-binding-site elements on translational efficiency in Bacillus subtilis and Escherichia coli in vivo. Mol Microbiol. 1992; 6:1105–1114. [PubMed: 1375309]

Weiss MS. Global indicators of X-ray data quality. J Appl Crystallogr. 2001; 34:130–135.

Weixlbaumer A, Jin H, Neubauer C, Voorhees RM, Petry S, Kelley AC, Ramakrishnan V. Insights into translational termination from the structure of RF2 bound to the ribosome. Science. 2008; 322:953–956. [PubMed: 18988853]

Wilson DN, Doudna Cate JH. The structure and function of the eukaryotic ribosome. Cold Spring Harb Perspect Biol. 2012; 4

Woese, CR. The present status of the genetic code. In: Davidson, N.; Cohn, WE., editors. Progress in Nucleic Acid Research and Molecular Biology. Academic Press; New York: 1967. p. 107-172.

Zaher HS, Green R. Quality control by the ribosome following peptide bond formation. Nature. 2009; 457:161–166. [PubMed: 19092806]

Zaher HS, Green R. Kinetic basis for global loss of fidelity arising from mismatches in the P-site codon:anticodon helix. RNA. 2010; 16:1980–1989. [PubMed: 20724456]

Zhang Z, Shah B, Bondarenko PV. G/U and certain wobble position mismatches as possible main causes of amino acid misincorporations. Biochemistry. 2013; 52:8165–8176. [PubMed: 24128183]

Zoll J, Tessari M, Van Kuppeveld FJ, Melchers WJ, Heus HA. Breaking pseudo-twofold symmetry in the poliovirus 3′-UTR Y-stem by restoring Watson-Crick base pairs. RNA. 2007; 13:781–792. [PubMed: 17449731]

Highlights

- Crystal structure of the 70S ribosome with tRNA^{fMet} interacting with the AUC codon

- Cytosine-Cytosine wobble mismatch in the P site forms a nearly coplanar base pair

- The P site stabilizes a normally disruptive C-C mismatch in the initiation complex

- mRNA conformation in the A and P sites is similar to those in cognate 70S complexes
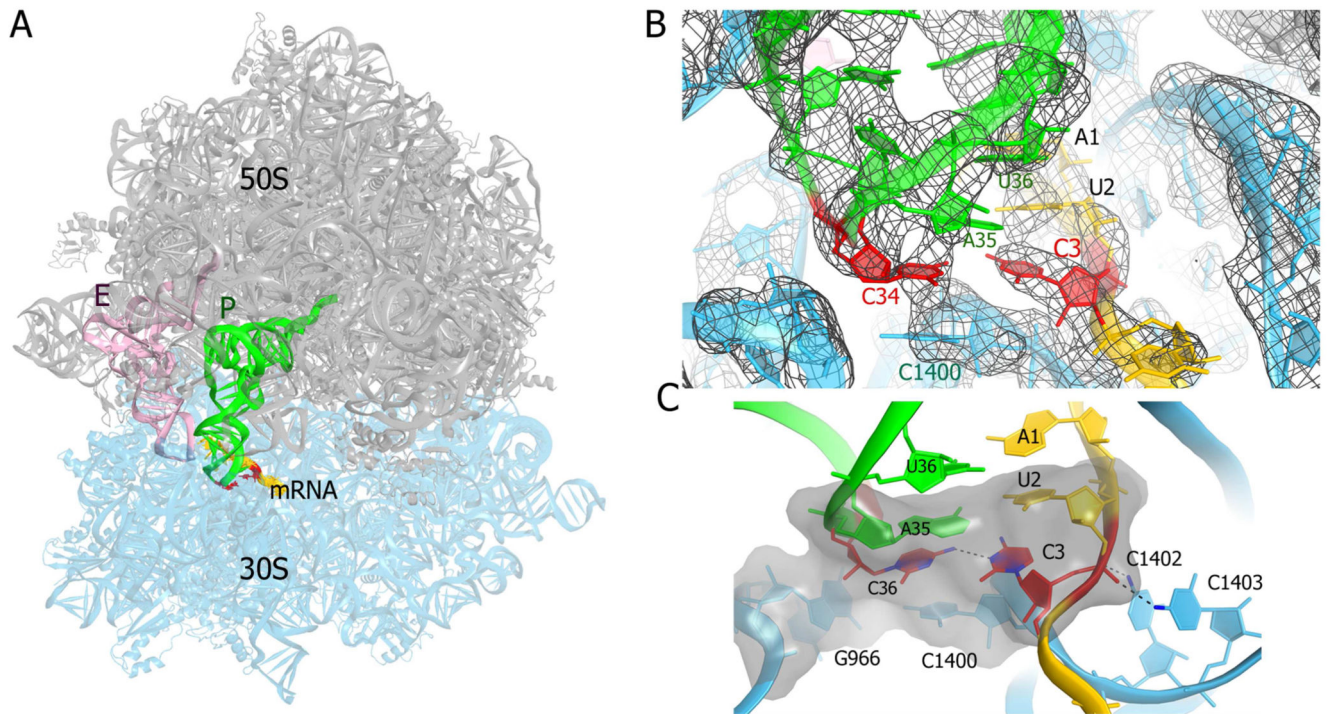
Figure 1.
Crystal structure of the *T. th.* 70S ribosome containing a C-C mismatch in the wobble position of the P site. (A) The ribosome crystal structure. The subunits are shown in gray (50S) and cyan (30S); mRNA is yellow, P-site tRNA is green and E-site tRNA is pink. The C-C mismatch is highlighted by red color. (B) 2Fo-Fc electron density (gray mesh) for the ribosomal P site. The colors of the structural model are as in panel A. (C) The packing and hydrogen-bonding interactions that stabilize the C-C mismatch. The van der Waals surface (gray) shows stacking interactions of the C-C pair (red) with the second codon-anticodon pair and ribosomal nucleotides C1400 and G966.
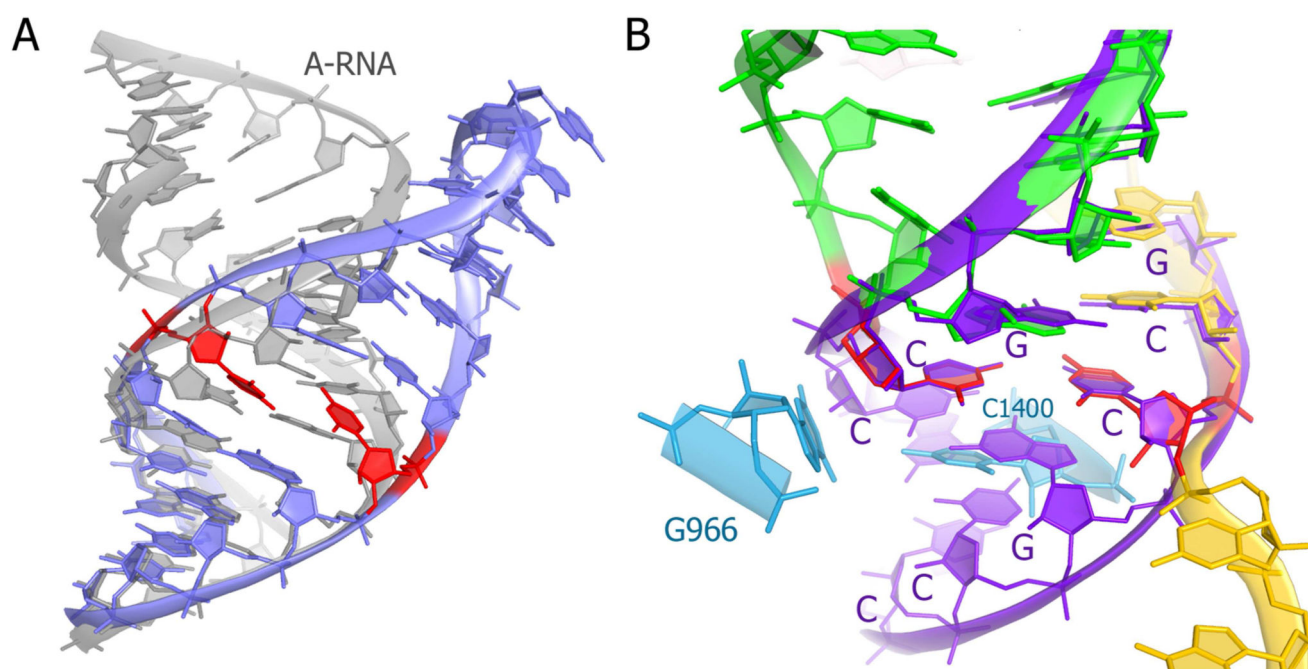
Figure 2.
The effect of the C-C mismatch on RNA structure. (A) Solution NMR structure (slate blue) of an RNA hairpin containing a C-C mismatch (PDB ID 2RPT; (Tavares et al., 2009)) shows that the cytosines (red) deviate from co-planarity and induce a large deviation of RNA conformation from that of an A-form double helix (gray). (B) The C-C mismatch (red) in the 70S P site does not disrupt the A-form RNA geometry of the codon-anticodon helix, which resembles the (CCG)$_n$-repeat double helix (purple; PDB ID 4E59; (Kiliszek et al., 2012)). In the (CCG)n-repeat double helix, the C-C mismatch is stabilized by interactions with the flanking G-C pairs, which are part of the crystal-lattice-stabilized system of the stacked base pairs. 16S rRNA is cyan; mRNA is yellow, P-site tRNA is green with the exception of the C-C mismatch, which is shown in red.
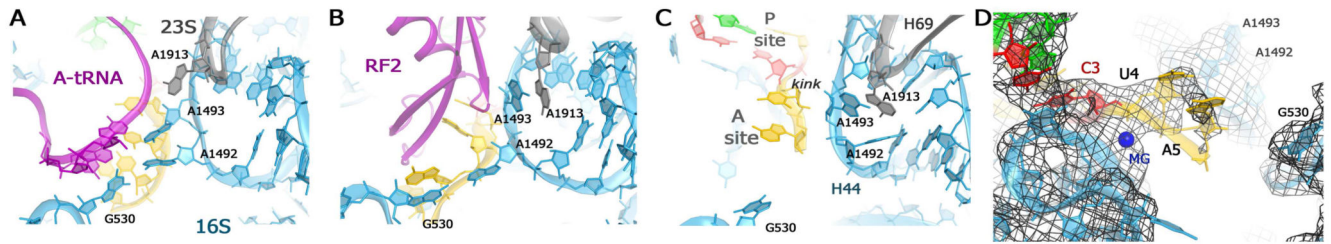
Figure 3.
Comparison of 70S ribosome crystal structures showing the ribosomal A site (decoding center) in the presence of cognate tRNA, release factor RF2 or the preceding P-site C-C mismatch. In panels A–D, 23S ribosomal RNA is shown in gray, 16S rRNA in cyan; mRNA in yellow, P-site tRNA in green. The C-C mismatch is indicated in red (panels C and D). (A) Conformation of the decoding center in the presence of cognate tRNA^{Phe} (magenta) bound to the A site (PDB ID 2J00; (Selmer et al., 2006)). (B) Conformation of the decoding center in the presence of release factor RF2 (magenta) bound in response to a UAA stop codon (PDB ID 3F1E; (Korostelev et al., 2008)). (C) Conformation of the vacant decoding center in the 70S C-C mismatch complex (this work). (D) Fo-Fc simulated-annealing omit map (gray) shows unbiased density of the decoding center (this work).

Table 1

Data collection and structure refinement statistics

Data collection	
Space group	$P2_12_12_1$
Cell dimensions	
a, b, c (Å)	211.72, 452.97, 620.15
α, β, γ (°)	90, 90, 90
Resolution (Å)	3.63 (3.63 – 3.83)[*]
$R_{\text{p.i.m}}$[#]	0.24 (1.6)
$CC(1/2)$[##]	99.7 (42.6)
$I/\sigma I$	5.7 (1.0)
Completeness (%)	99.3 (99.3)
Redundancy	10.5 (10.5)
Structure Refinement	
Resolution (Å)	60 – 3.63
No. reflections	661200
$R^{\text{work}} / R^{\text{free}}$	0.268 / 0.287
Total No. atoms	295,628
Ions/water (modeled as Mg^{2+})	2218
R.m.s. deviations	
Bond lengths (Å)	0.002
Bond angles (°)	0.542

[*] Values in parentheses are for the high-resolution shell.

[#] $R_{\text{p.i.m}}$ (precision-indicating merging R factor (Weiss, 2001), was calculated using SCALA, which is part of CCP4 package (1994)

[##] CC(1/2) is the percentage of correlation between intensities from random half-datasets as defined by Karplus and Diederichs (Karplus and Diederichs, 2012)